

The distribution and generation of carbonatites

Sally Gibson*, Dan McKenzie, and Sergei Lebedev
Department of Earth Sciences, University of Cambridge, UK

ABSTRACT

The physio-chemical framework that generates carbonatites and, ultimately, the associated rare earth element deposits remains contentious. This primarily reflects the diverse tectonic settings in which carbonatites occur: large igneous provinces, continental rifts and major extensional terranes, syn- to post-collisional settings, or ocean islands. There is, however, a broad consensus that carbonatites (or their parental melts) originate in the mantle. These exotic melts have small volumes that make them ideal probes of conditions in their underlying source regions. We combine the carbonatite locations with global maps of lithospheric thickness, derived from seismic tomography, and show that post-Neoproterozoic carbonatites occur preferentially above the margins of thick cratonic lithosphere (e.g., adjacent to the South Atlantic and Indian Oceans or in North America, Greenland, and Asia) and where once thick lithosphere has undergone stretching (e.g., eastern Asia). Our thermal modeling reveals that lateral and vertical heat conduction on rifted craton margins, or rapid stretching of cratonic lithosphere, can mobilize carbonated peridotite at the temperatures (950–1250 °C) and pressures (2–3 GPa) required to form primary carbonatites or their parental alkali silicate melts. Importantly, our models show that heat conduction from upwelling mantle plumes or ambient mantle on rifted cratonic margins may sufficiently modify the temperature of the lithospheric mantle to cause melting of carbonated peridotite, settling the long-standing debate on the role of rifting and heating in the generation of carbonatites.

INTRODUCTION

Carbonatites and their associated alkali-silicate melts host the majority of primary rare earth element (REE) deposits (e.g., Chakhmouradian and Wall, 2012). In addition to their economic significance, carbonatites are exceptionally rich in CO₂ (>25 wt%) and play an important role in the deep cycling of carbon (e.g., Foley and Fischer, 2017). Despite the increasing scientific and economic interest, a physio-chemical framework to account for the global distribution of carbonatites is controversial, and the relative roles of rifting and mantle plumes in the generation of carbonatites have been vigorously debated for more than 60 years. The contention primarily arises because of: (i) their extreme reactivity, which makes their initial composition difficult to reconstruct (see Yaxley et al., 2022); and (ii) occurrence in diverse tectonic settings, i.e., large igneous provinces (LIPs),

rift zones and extensional terranes, subduction and collision zones, and ocean islands (Bailey, 1964; Le Bas, 1984; Gibson et al., 2006; Bell and Simonetti, 2010; Ernst, 2014; Hou et al., 2015; Goodenough et al., 2021; Zhang et al., 2022).

Small-fraction volatile-rich melts, such as carbonatites, lamprophyres, and kimberlites are thought to be emplaced in the crust immediately above their mantle source regions and therefore act as probes of conditions in the underlying mantle at the time of their formation (e.g., Gibson et al., 1993). Previous investigations have shown that 88% of all dated carbonatites are in Precambrian cratons (Woolley and Bailey, 2012) and within 600 km of their edges (e.g., Humphreys-Williams and Zahirovic, 2021). Maps from seismic tomographic models show, however, that while many large-scale geological features are the surface expression of structures that extend through the whole lithosphere, they often differ in lateral extent at sub-crustal depths (e.g., Priestley and McKenzie, 2006; Afonso et al., 2022; Hou et al., 2023). Here we

exploit recent increases in the global seismic coverage and resolution of seismic tomographic models, which more precisely define the margins of cratonic lithosphere. We show how these—together with the thermal structure and composition of Earth's lithospheric mantle—control the genesis of many Neoproterozoic to Recent carbonatites.

METHODS

Tomographic inversion based on waveforms or on global measurements of the phase velocities of Love and Rayleigh waves, and especially those of higher mode velocities, can be used to construct three-dimensional models of upper mantle shear wave velocities (V_s). In general, the resulting maps agree well, and their resolution has improved steadily. From a geological point of view, it is temperature (T) rather than V_s that is of interest. The V_s - T relationship at seismic frequencies cannot be measured directly, but must be calculated from the shear modulus determined from forced oscillations at the relevant periods. Priestley et al. (2024) combined the values of shear modulus from recent laboratory experiments with seismological estimates of V_s from regions where the T and pressure (P) can be estimated from petrological and geophysical arguments to obtain an empirical expression for $T(V_s, P)$ for peridotite, the most common lithology in the mantle. A similar parameterization for the V_s model of Schaeffer and Lebedev (2013) shows that the temperature variations in the mantle estimated from seismic tomography are similar and now reasonably well constrained (see Supplemental Material¹).

A common method of representing three-dimensional temperature models is to use them to estimate lithospheric thickness. The definition of lithospheric thickness used here is the depth at which the extrapolation of the shallow conductive part of the geotherm reaches an isentropic potential temperature (T_p) for the upper mantle, which we assume to be 1315 °C (Priestley and

Sally Gibson  <https://orcid.org/0000-0002-4835-2908>
*sally@esc.cam.ac.uk

¹Supplemental Material. Description of methods (File S1) and the numerical code for the thermal model. The data sets are available in Files S2 and S3, and the Fortran code is available in Files S4 and S5. Please visit <https://doi.org/10.1130/GEOL.S.25988053> to access the supplemental material; contact editing@geosociety.org with any questions.

McKenzie, 2006). In order to elucidate the relationship with carbonatites, we have superimposed their locations (Woolley and Kjarsgaard, 2008; Liu et al., 2023) on global maps of lithospheric thickness.

GLOBAL DISTRIBUTIONS OF CARBONATITES AND SEISMIC TOMOGRAPHY

Global maps of lithospheric thickness derived from seismic tomography reveal that the cores of the major continents have thick roots extending to depths of >200 km (Schaeffer and Lebedev, 2013; Afonso et al., 2022; Hou et al., 2023; Priestley et al., 2024). Important for our study are the boundaries of major Archean cratons; here, we consider cratons as regions where the lithosphere extends to depths >160 km and have been tectonically stable for the past 2.5 Ga. The world's oldest carbonatites (ca. 3 Ga) occur in west Australia, Canada, and southern Greenland (Fig. 1) above thick lithosphere and adjacent to sutures of Archean crustal blocks (Fig. S6). The tectonic setting at the time of their emplacement and also many Mesoproterozoic and Paleoproterozoic carbonatites, including those with economic REE deposits at Bayan Obo and Mountain Pass, which are associated with LIPs and the break-up of the Nuna supercontinent (Zhang et al., 2022), remains unclear. To negate the effects of post melt generation tectonic processes, our study is primarily focused on carbonatites that post-date the major plate

reorganization linked with the break-up of Pangaea ca. 200 Ma, together with those that formed earlier in the Phanerozoic and Neoproterozoic.

Previous studies have noted the occurrence of carbonatites on the margins of outcrops of Precambrian crustal blocks (Hou et al., 2015; Humphreys-Williams and Zahirovic, 2021). A key observation from Figure 1 is that the locations of carbonatites are influenced by the whole lithospheric structure (i.e., crust and mantle), and Figure 2 shows that they lie above where there are major changes in the gradient at the base of the lithosphere, i.e., on the margins of thick cratonic lithosphere. This is especially the case for Phanerozoic and Neoproterozoic carbonatites associated with rifting and the formation of the Atlantic and Indian Oceans. Many carbonatites emplaced in the past 1 Ga in south and central Africa, North America (Fig. 2), and some of those in eastern Asia are also near major changes in present-day lithospheric thickness (Fig. 1). A few carbonatites occur in regions of thin (<100 km) continental lithosphere that has undergone large amounts of extension (e.g., eastern China).

While the horizontal resolution of the seismic tomography does not reveal structures with widths <100 km (e.g., Malawi and Kontozero Rifts) it is clear from the lithospheric thickness profiles for Africa, South America, and North America in Figures 2D, 2E, and 2F that the boundaries of the major cratons are well defined and have the steep gradients. Moreover, many

young (<200 Ma) carbonatites on the continental margins in the Atlantic realm lie between thin oceanic and thick cratonic lithosphere, through which diamond-bearing kimberlites were emplaced (Figs. 2D, 2E, and 2F). Numerous of these carbonatites are associated with LIPs linked to impacting mantle plumes (e.g., Deccan, Karoo, Paraná-Etendeka, Alto Paranaíba, Central and North Atlantic magmatic provinces; Gibson et al., 1995; Ernst, 2014) and immediately pre-date or are synchronous with continental break-up, having similar ages to those of the oldest adjacent sea floor. The presence of carbonatites along the Eastern and Western branches of the East African Rift (e.g., Oldoinyo Lengai) also shows they can be produced by limited extension above a high-temperature thermal anomaly (e.g., Ebinger and Sleep, 1998). But some carbonatites post-date break-up by tens of millions of years (e.g., on the southern coastal margin of Brazil) and have no obvious relationship with hotspots.

GENERATION OF CO₂-RICH MANTLE MELTS

Carbonatites require specific conditions in the mantle for their formation. They may be generated by incipient, high pressure (>6 GPa) melting of carbonated peridotite in the convecting mantle (Dasgupta and Hirschmann, 2006), but only a few carbonatites have high ³He/⁴He ratios indicative of a primordial mantle component (Bell and Simonetti, 2010) or δ¹¹B and

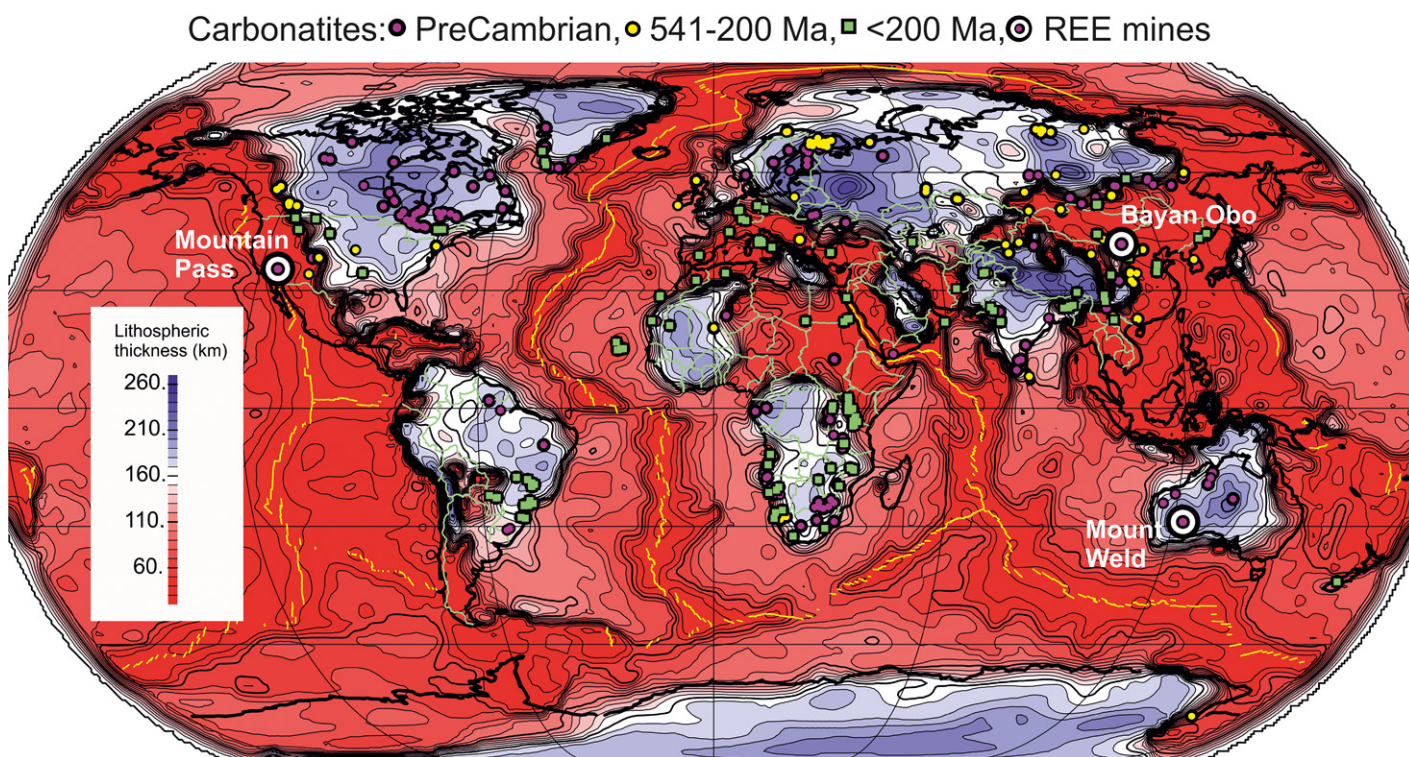


Figure 1. Global map of lithospheric thickness (Priestley et al., 2024) with locations of carbonatites (Woolley and Kjarsgaard, 2008; Liu et al., 2023). REE—rare earth element.

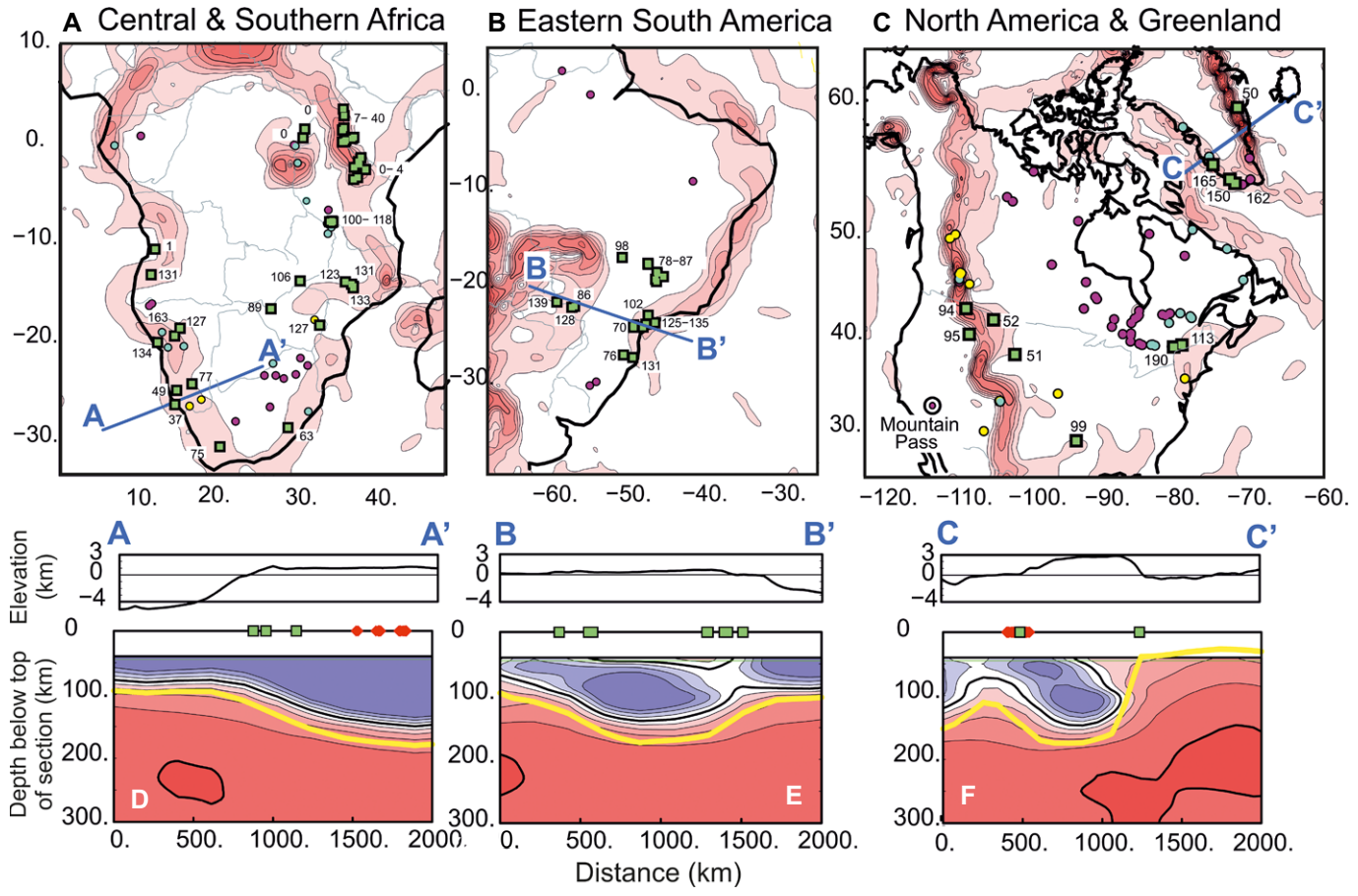


Figure 2. Maps of (A) central and southern Africa, (B) eastern South America, and (C) North America showing gradients at the base of the lithosphere, based on the seismic tomography model of Priestley et al. (2024), together with the distributions of carbonatites (Liu et al., 2023). (D–F) Profiles of lithospheric temperatures along lines of sections shown on the corresponding maps. Kimberlite locations on profiles are taken from Giuliani and Pearson (2019).

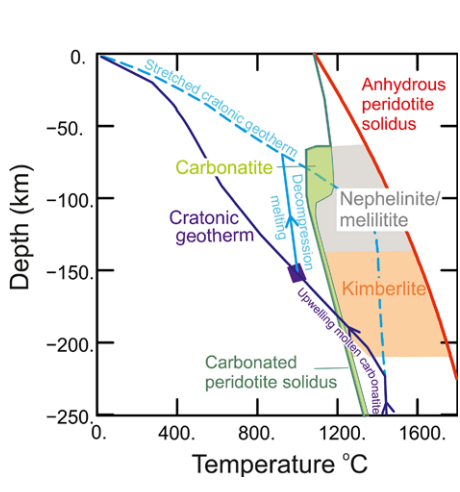


Figure 3. Experimental studies show that carbonatites and their parental melts (melilitites and nephelinites) are generated at specific conditions in the mantle (Pintér et al., 2021). An important region lies between 2–3 GPa and 950–1300 °C. Conductive geotherms associated with lithosphere between 75 and 150 km thick intersect this region. The cratonic geotherm was calculated for a 200-km-thick lithosphere and assumes a crustal thickness of 40 km.

$\delta^{34}\text{S}$ isotopes that resemble convecting upper mantle melts (e.g., Hutchison et al., 2019; Kuebler et al., 2020). Instead, $\delta^{11}\text{B}$ and $\delta^{34}\text{S}$ isotopes indicate recycled crustal components in mainly Phanerozoic carbonatites; some of these may represent shallow (1–3 GPa) melts of subducted limestones with mantle peridotite (Chen et al., 2023). These and other carbonate-peridotite-derived melts are likely to remain interconnected at small melt fractions (Hunter and McKenzie, 1989), be expelled from the asthenosphere, and ascend into the lithosphere. But their movement is too slow, and the volumes too small, to perturb the temperature (McKenzie, 1989), and the upwelling melt will solidify at a depth where the steady-state geotherm is at the carbonated peridotite solidus, i.e., at a temperature of 950–1100 °C and between 2 and 3 GPa (depths of 65–100 km, e.g., Wallace and Green, 1988; Pintér et al., 2021; Fig. 3). Incipient melting of this metasomatized (CO_2 -bearing) peridotite will generate carbonatites (e.g., Wallace and Green, 1988). At similar pressures but higher temperatures, carbonated peridotite melts to form CO_2 -rich silicate melts that may ascend and evolve to form carbonatites during shallow

(0.1–1 GPa) crustal processing. This may be via immiscibility from an olivine melilitite (Kjarsgaard et al., 1995) or extensive differentiation of olivine nephelinites (Watkinson and Wylie, 1971). Carbonated peridotite in the lithospheric mantle between 2 and 3 GPa is therefore a “sweet spot” for the generation of carbonatites if it can be mobilized.

THERMAL MODELS FOR CARBONATITE FORMATION

The repetition of carbonatite emplacement in the same region, sometimes billions of years apart (e.g., East Africa and Gardar Rifts) has been used to infer ambient mantle temperatures (Woolley and Kjarsgaard, 2008; Woolley and Bailey, 2012). Nevertheless, ocean islands with carbonatites (e.g., Canary, Cape Verde, and Kerguelen) are all linked to mantle plumes. Below we attempt to shed new light on the basic underlying processes that generate carbonatites by combining our observations with the results of published lab experiments and new thermal modeling.

The most substantial amounts of solid carbonate are likely to accumulate within thick,

Downloaded from <http://pubs.geoscienceworld.org/gsa/geology/article-pdf/doi/10.1130/G52141.1/6519734/g52141.pdf> by University of Cambridge user

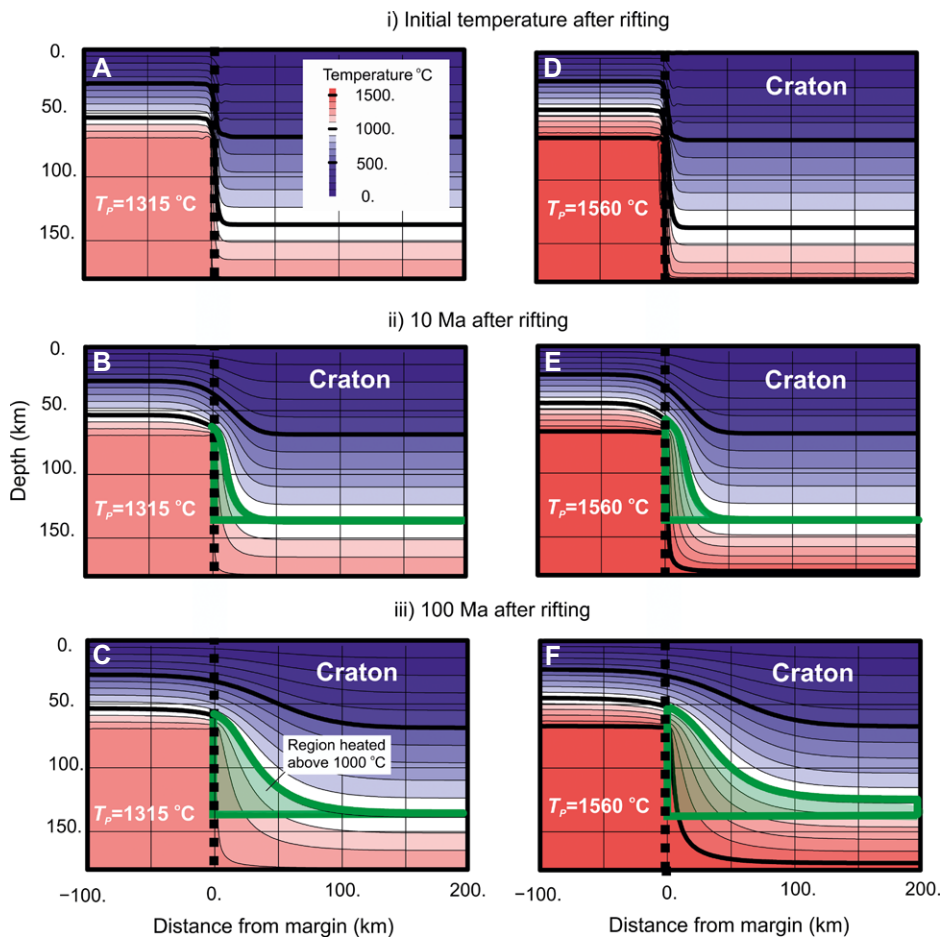


Figure 4. Simple model of the thermal evolution of a craton boundary to illustrate the effects of rifting and heating events at craton margins. Green shading shows the region of generation of carbonatites or their parental magmas (i.e., nephelinites or melilitites). The examples illustrate temperature variations in the lithosphere adjacent to a craton that has been stretched to a thickness of 70 km and at various times (0–100 Ma) after both passive (A–C) and active rifting (D–F).

cold, ancient cratonic lithosphere where there is the greatest time for metasomatism either related to subduction (e.g., Hou et al., 2023) or small-fraction melts derived from the underlying convecting mantle (McKenzie, 1989). There are two obvious ways in which to mobilize carbonated peridotite in the cratonic mantle. If the lithosphere is stretched, the carbonated peridotite will ascend to lower pressure where the temperature will exceed its solidus (Fig. 3). This behavior requires stretching to be sufficiently fast for the upwelling to occur approximately isentropically, without substantial heat loss to the surface by conduction. This may explain the carbonatites in eastern Asia (Fig. 1) that occur on lithosphere that has undergone extensive thinning, i.e., the North China craton.

The other scenario involves rifting adjacent to cratonic lithosphere. Whether and how upwelling mantle heats the colder cratonic lithosphere will depend on its geometry. The density of depleted cratonic mantle is $\sim 60 \text{ kg m}^{-3}$ less than the convecting upper mantle (e.g., Poudjom Djomani et al., 2001). If the upwelling hot mantle

is $500 \text{ }^\circ\text{C}$ hotter than the cratonic mantle, they will have approximately the same density. Under these conditions, a vertical boundary between the upwelling hot mantle and cold depleted lithosphere will be mechanically stable. These arguments suggest that a model with vertical boundaries can provide a simple scenario for the thermal evolution of such rifted boundaries.

Our new thermal models (see Fig. 4 and Supplemental Material) show that if the lithosphere adjacent to a craton is rifted and thinned to a depth of 70 km, lateral conduction of heat from ambient mantle ($T_p = 1315 \text{ }^\circ\text{C}$) will raise the temperature in substantial regions of the cratonic lithosphere within 25 km of the rift zone. This will be above the solidus of carbonated peridotite between depths of 60–140 km (Figs. 4A, 4B, and 4C), which is where experiments show that primary carbonatites and their parental melts will form (i.e., olivine melilitites and nephelinites; Fig. 3). Figures 4D, 4E, and 4F show the corresponding behavior above a mantle plume with a T_p of $1560 \text{ }^\circ\text{C}$. This leads to more extensive remobilization of carbonated perido-

lite at a horizontal distance of 30 km from the rifted margin, by lateral heat conduction from the mantle plume between a maximum depth interval of 50–140 km, and also by vertical heat conduction through the base of the cratonic lithosphere between a narrower depth interval (120 and 100 km) distal to the rift zone. The model also shows that the temperature of a substantial region of cratonic mantle is raised above the carbonated peridotite solidus in the first 10 m.y. of stretching and heating.

CONCLUSIONS

High-resolution seismic models, together with compilations of the locations and ages of global carbonatites, have allowed us to refine the extent to which the temperature, composition, and thickness of Earth's lithosphere control the distribution of these enigmatic magmas. Many Neoproterozoic and Phanerozoic carbonatites are concentrated in extensional terranes or around steeply dipping craton margins.

The results of our simple thermal models are consistent with our present understanding of melt movement in the mantle, the steady-state temperature structure of cratons, and temperature changes resulting from rifting and stretching. They reveal that at rifted craton margins, carbonated peridotitic mantle can be mobilized to form primary carbonatites (or their parental magmas) by lateral and vertical heat conduction. This may be from upwelling of mantle at both ambient and high mantle temperatures and hence sheds new light on the long-standing controversy on the role of continental rifting and mantle plumes in the generation of carbonatites. Rapid stretching of thick lithospheric mantle containing carbonated peridotite may also lead to the formation of these exotic melts (e.g., eastern Asia). If our models are correct, carbonatites could contain very large and variable concentrations of incompatible trace elements. In order to form economic deposits of REEs, however, it is necessary for these elements to be further concentrated by evolution of residual liquids (e.g., Bayan Obo; Kuebler et al., 2020), hydrothermal processes, or weathering (e.g., Mount Weld; Anenburg et al., 2021). More work is now required to understand the distributions of Mesoproterozoic and Paleoproterozoic carbonatites and also Archean carbonatites, which occur in regions where the underlying lithosphere is $>150 \text{ km}$ thick at the present day.

ACKNOWLEDGEMENTS

We are grateful to K. Goodenough and an anonymous reviewer for their comments on an earlier draft of the manuscript. This work was funded by Natural Environment Research Council grants NE/Y000218/1 and XE/X000060/1.

REFERENCES CITED

Afonso, J.C., et al., 2022, Thermochemical structure and evolution of cratonic lithosphere in central

- and southern Africa: *Nature Geoscience*, v. 15, p. 405–410, <https://doi.org/10.1038/s41561-022-00929-y>; erratum available at <https://doi.org/10.1038/s41561-023-01124-3>.
- Anenburg, M., Broom-Fendley, S., and Chen, W., 2021, Formation of rare earth deposits in carbonatites: *Elements*, v. 17, p. 327–332, <https://doi.org/10.2138/gselements.17.5.327>.
- Bailey, D.K., 1964, Crustal warping—a possible tectonic control of alkaline magmatism: *Journal of Geophysical Research* (1896–1977), v. 9, p. 1103–1111, <https://doi.org/10.1029/JZ069i006p01103>.
- Bell, K., and Simonetti, A., 2010, Source of parental melts to carbonatites—critical isotopic constraints: *Mineralogy and Petrology*, v. 98, p. 77–89, <https://doi.org/10.1007/s00710-009-0059-0>.
- Chakhmouradian, A.R., and Wall, F., 2012, Rare earth elements: Minerals, mines, magnets (and more): *Elements*, v. 8, p. 333–340, <https://doi.org/10.2113/gselements.8.5.333>.
- Chen, W., Zhang, G., Keshav, S., and Li, Y., 2023, Pervasive hydrous carbonatitic liquids mediate transfer of carbon from the slab to the subarc mantle: *Communications Earth & Environment*, v. 4, 73, <https://doi.org/10.1038/s43247-023-00741-5>.
- Dasgupta, R., and Hirschmann, M.M., 2006, Melting in the Earth's deep upper mantle caused by carbon dioxide: *Nature*, v. 440, p. 659–662, <https://doi.org/10.1038/nature04612>.
- Ebinger, C.J., and Sleep, N.H., 1998, Cenozoic magmatism throughout east Africa resulting from impact of a single plume: *Nature*, v. 395, p. 788–791, <https://doi.org/10.1038/27417>.
- Ernst, R.E., 2014, Links with carbonatites, kimberlites, and lamprophyres/lamproites, *in* Ernst, R.E., ed., *Large Igneous Provinces*: Cambridge, Cambridge University Press, p. 245–276, <https://doi.org/10.1017/CBO9781139025300.009>.
- Foley, S.F., and Fischer, T.P., 2017, An essential role for continental rifts and lithosphere in the deep carbon cycle: *Nature Geoscience*, v. 10, p. 897–902, <https://doi.org/10.1038/s41561-017-0002-7>.
- Gibson, S.A., Thompson, R.N., Leat, P.T., Morrison, M.A., Hendry, G.L., Dickin, A.P., and Mitchell, J.G., 1993, Ultrapotassic magmas along the flanks of the Oligo-Miocene Rio Grande Rift, USA: Monitors of the zone of lithospheric mantle extension and thinning beneath a continental rift: *Journal of Petrology*, v. 34, p. 187–228, <https://doi.org/10.1093/ptrology/34.1.187>.
- Gibson, S.A., Thompson, R.N., Leonardos, O.H., Dickin, A.P., and Mitchell, J.G., 1995, The Late Cretaceous impact of the Trindade mantle plume: Evidence from large-volume, mafic, potassic magmatism in SE Brazil: *Journal of Petrology*, v. 36, p. 189–229, <https://doi.org/10.1093/ptrology/36.1.189>.
- Gibson, S.A., Thompson, R.N., and Day, J.A., 2006, Timescales and mechanisms of plume–lithosphere interactions: $^{40}\text{Ar}/^{39}\text{Ar}$ geochronology and geochemistry of alkaline igneous rocks from the Paraná–Etendeka Large Igneous Province: *Earth and Planetary Science Letters*, v. 251, p. 1–17, <https://doi.org/10.1016/j.epsl.2006.08.004>.
- Giuliani, A., and Pearson, D.G., 2019, Kimberlites: From deep earth to diamond mines: *Elements*, v. 15, p. 377–380, <https://doi.org/10.2138/gselements.15.6.377>.
- Goodenough, K.M., Deady, E.A., Beard, C.D., Broom-Fendley, S., Elliott, H.A.L., van den Berg, F., and Öztürk, H., 2021, Carbonatites and alkaline igneous rocks in post-collisional settings: Storehouses of rare earth elements: *Journal of Earth Science*, v. 32, p. 1332–1358, <https://doi.org/10.1007/s12583-021-1500-5>; erratum available at <https://doi.org/10.1007/s12583-022-1312-2>.
- Hou, Z., Liu, Y., Tian, S., Yang, Z., and Xie, Y., 2015, Formation of carbonatite-related giant rare-earth-element deposits by the recycling of marine sediments: *Scientific Reports*, v. 5, <https://doi.org/10.1038/srep10231>.
- Hou, Z.-Q., et al., 2023, Refertilized continental root controls the formation of the Mianning–Dechang carbonatite-associated rare-earth-element ore system: *Communications Earth & Environment*, v. 4, 293, <https://doi.org/10.1038/s43247-023-00956-6>.
- Humphreys-Williams, E.R., and Zahirovic, S., 2021, Carbonatites and global tectonics: *Elements*, v. 17, p. 339–344, <https://doi.org/10.2138/gselements.17.5.339>.
- Hunter, R.H., and McKenzie, D., 1989, The equilibrium geometry of carbonate melts in rocks of mantle composition: *Earth and Planetary Science Letters*, v. 92, p. 347–356, [https://doi.org/10.1016/0012-821X\(89\)90059-9](https://doi.org/10.1016/0012-821X(89)90059-9).
- Hutchison, W., Babiak, R.J., Finch, A.A., Marks, M.A.W., Markl, G., Boyce, A.J., Stüeken, E.E., Friis, H., Borst, A.M., and Horsburgh, N.J., 2019, Sulphur isotopes of alkaline magmas unlock long-term records of crustal recycling on Earth: *Nature Communications*, v. 10, 4208, <https://doi.org/10.1038/s41467-019-12218-1>.
- Kjarsgaard, B.A., Hamilton, D.L., and Peterson, T.D., 1995, Peralkaline nephelinite/carbonatite liquid immiscibility: Comparison of phase compositions in experiments and natural lavas from Oldoinyo Lengai, *in* Bell, K., and Keller, J., eds., *Carbonatite Volcanism: Oldoinyo Lengai and the Petrogenesis of Natrocarbonatites*: Berlin, Heidelberg, Springer, IAVCEI Proceedings in Volcanology, v. 4, p. 163–190, https://doi.org/10.1007/978-3-642-79182-6_13.
- Kuebler, C., Simonetti, A., Chen, W., and Simonetti, S.S., 2020, Boron isotopic investigation of the Bayan Obo carbonatite complex: Insights into the source of mantle carbon and hydrothermal alteration: *Chemical Geology*, v. 557, <https://doi.org/10.1016/j.chemgeo.2020.119859>.
- Le Bas, M.J., 1984, Oceanic carbonatites, *in* Kornprobst, J., ed., *Kimberlites—I: Kimberlites and Related Rocks*: Elsevier, Developments in Petrology, v. 11, part A, p. 169–178, <https://doi.org/10.1016/B978-0-444-42273-6.50020-1>.
- Liu, S.-L., Ma, L., Zou, X., Fang, L., Qin, B., Melnik, A.E., Kirscher, U., Yang, K.-F., Fan, H.-R., and Mitchell, R.N., 2023, Trends and rhythms in carbonatites and kimberlites reflect thermo-tectonic evolution of Earth: *Geology*, v. 51, p. 101–105, <https://doi.org/10.1130/G50775.1>.
- McKenzie, D., 1989, Some remarks on the movement of small melt fractions in the mantle: *Earth and Planetary Science Letters*, v. 95, p. 53–72, [https://doi.org/10.1016/0012-821X\(89\)90167-2](https://doi.org/10.1016/0012-821X(89)90167-2).
- Pintér, Z., Foley, S.F., Yaxley, G.M., Rosenthal, A., Rapp, R.P., Lanati, A.W., and Rushmer, T., 2021, Experimental investigation of the composition of incipient melts in upper mantle peridotites in the presence of CO₂ and H₂O: *Lithos*, v. 396–397, <https://doi.org/10.1016/j.lithos.2021.106224>.
- Poudjom Djomani, Y.H., O'Reilly, S.Y., Griffin, W.L., and Morgan, P., 2001, The density structure of subcontinental lithosphere through time: *Earth and Planetary Science Letters*, v. 184, p. 605–621, [https://doi.org/10.1016/S0012-821X\(00\)00362-9](https://doi.org/10.1016/S0012-821X(00)00362-9).
- Priestley, K., and McKenzie, D., 2006, The thermal structure of the lithosphere from shear wave velocities: *Earth and Planetary Science Letters*, v. 244, p. 285–301, <https://doi.org/10.1016/j.epsl.2006.01.008>.
- Priestley, K., Ho, T., Takei, Y., and McKenzie, D., 2024, The thermal and anisotropic structure of the top 300 km of the mantle: *Earth and Planetary Science Letters*, v. 626, <https://doi.org/10.1016/j.epsl.2023.118525>.
- Schaeffer, A.J., and Lebedev, S., 2013, Global shear speed structure of the upper mantle and transition zone: *Geophysical Journal International*, v. 194, p. 417–449, <https://doi.org/10.1093/gji/ggt095>.
- Wallace, M.E., and Green, D.H., 1988, An experimental determination of primary carbonatite magma composition: *Nature*, v. 335, p. 343–346, <https://doi.org/10.1038/335343a0>.
- Watkinson, D.H., and Wyllie, P.J., 1971, Experimental study of the composition join NaAlSi₃O₈–CaCO₃–H₂O and the genesis of alkalic rock—Carbonatite complexes: *Journal of Petrology*, v. 12, p. 357–378, <https://doi.org/10.1093/ptrology/12.2.357>.
- Woolley, A.R., and Bailey, D.K., 2012, The crucial role of lithospheric structure in the generation and release of carbonatites: geological evidence: *Mineralogical Magazine*, v. 76, p. 259–270, <https://doi.org/10.1180/minmag.2012.076.2.02>.
- Woolley, A.R., and Kjarsgaard, B.A., 2008, Paragenetic types of carbonatite as indicated by the diversity and relative abundances of associated silicate rocks: Evidence from a global database: *Canadian Mineralogist*, v. 46, p. 741–752, <https://doi.org/10.3749/canmin.46.4.741>.
- Yaxley, G.M., Anenburg, M., Tappe, S., Decree, S., and Guzmics, T., 2022, Carbonatites: Classification, sources, evolution, and emplacement: *Annual Review of Earth and Planetary Sciences*, v. 50, p. 261–293, <https://doi.org/10.1146/annurev-earth-032320-104243>.
- Zhang, S.-H., Ernst, R.E., Yang, Z., Zhou, Z., Pei, J., and Zhao, Y., 2022, Spatial distribution of 1.4–1.3 Ga LIPs and carbonatite-related REE deposits: Evidence for large-scale continental rifting in the Columbia (Nuna) supercontinent: *Earth and Planetary Science Letters*, v. 597, p. 117815, <https://doi.org/10.1016/j.epsl.2022.117815>.

Printed in the USA